Modeling velocity autocorrelation functions for confined fluids using γ distributions

S. H. Krishnan and K. G. Ayappa

Department of Chemical Engineering, Indian Institute of Science, Bangalore 560012, India

We propose a model for the short-time dynamics of fluids confined in slit-shaped pores. The model has been developed from the observation that the real lobe of the instantaneous normal mode density of states (INM DOS) closely follows a γ distribution. By proposing that the density of states of the confined fluid can be represented by a γ distribution, the resulting velocity autocorrelation function (VACF) is constructed such that it is accurate upto the fourth frequency moment. The proposed model results in an analytical expression for the VACF and relaxation times. The VACFs obtained from the model have been compared with the VACFs obtained from molecular dynamic simulations and INM analysis for fluids confined in slit-shaped pores over a wide range of confinement and temperatures. The model is seen to capture the short-time behavior of the VACF extremely accurately and in this region is superior to the predictions of the VACF obtained from the real lobe of the INM DOS. Although the model predicts a zero self-diffusivity, the predicted relaxation times are in better agreement with the molecular dynamics results when compared with those obtained from the INM theory.

I. INTRODUCTION

Molecularly confined fluids are encountered in a variety of processes such as adsorption, wetting, boundary lubrication, and heterogeneous catalysis. The strong interactions of the fluid molecules with the confining walls, result in an inhomogeneous fluid whose spatial distribution of particles alter the structural and dynamic properties of the fluid. The surface force apparatus,[1] which measures forces between molecularly thin films confined between two mica surfaces, has enhanced our understanding of the fluid structure and dynamics of such systems. In addition to the structural phenomenon of layering and its relation to the oscillatory solvation force,[2] dynamic surface force experiments are aimed at inferring the state of the confined fluid from the measured force response. Although some experiments indicate that the confined fluid can freeze,[3] others show that it is more likely to be in a glassy state.[4] Experimental techniques such as fluorescence correlation spectroscopy are now able to probe the dynamic state of the confined fluid within the framework of the surface force apparatus in a more direct fashion.[5] The geometry of the fluid confined in a surface force apparatus can be modeled as confinement between two infinite parallel surfaces also known as slit pores. Molecular dynamics (MD) simulations have been extensively used to obtain diffusion coefficients and structural properties of fluids confined in slit-shaped pores.[6–10] There have been few attempts to develop a theory for transport in strongly inhomogeneous fluids. Kinetic theory for dense gases have been extended to develop a theory for confined inhomogeneous fluids,[11,12] and have been successful in predicting the variations in diffusion coefficients as a function of pore width for fluids confined in pores with structureless (smooth) walls.[12,13] Recently, we have applied liquid state theories based on the memory equation which seek to obtain the time correlation functions of fluids confined in slit-shaped pores.[14]

In this paper we apply instantaneous normal mode (INM) analysis[15–17] to study the dynamics of confined fluids. The basic notion underlying INM analysis is that the evolution of a system of interacting particles in phase space can at any instant approximated to be harmonic. A normal mode analysis of the trajectory involves expanding the potential energy of the system upto a quadratic term with respect to any instantaneous configuration. The ensemble averaged distribution of frequencies obtained from the normal mode analysis is referred to as the INM density of states (DOS), henceforth referred to as INM DOS. Owing to the fact that any arbitrary configuration of a liquid is not in a potential minima, the INM DOS contains both real (stable) and imaginary (unstable) modes. Although the velocity autocorrelation function (VACF) predicted from the complete INM DOS is divergent, it has been shown that[18] by discarding the imaginary modes in the INM DOS, one can predict the VACF for longer times with sufficient accuracy. It is well established that INMs can represent short-time dynamics of liquids accurately,[15] and in this regard has been very successful and complete in its applicability. However, the extension of the theory to predict long-time diffusive behavior is still under debate.[19–22] Although INMs have been used extensively to study the dynamics of bulk fluids and to a lesser extent in clusters, only few studies have extended these ideas to fluids confined in nanopores. INMs have recently been used to study the dynamics of rare gases confined in zeolites.[23,24] Since INMs provide an exact representations of short-time dynamics, and are known to perform well for systems when the dynamics is slower, it appears that the INM approach might be better suited to studying the dynamics of strongly

inhomogeneous fluids such as fluids confined in slit-shaped pores. To our knowledge INMs have not been applied to such systems.

Our objectives in this paper are twofold: We first obtain the INM DOS for a fluid confined in a slit-shaped pore and compare the predicted VACFs with those obtained from MD simulations for various degrees of confinement. From the observation that the real lobe of the INM DOS can be accurately represented as γ distributions we propose that the DOS of the system can be suitably modeled by a γ distribution. Although this proposition is unable to predict the long-time diffusive nature of the system, the utility of the model is checked by the ability to accurately predict the VACF at short and intermediate times. By requiring that the resulting VACF is accurate upto the fourth moment the two parameters of the γ distribution are expressed in terms of the second and the fourth frequency moments. Since the moments are obtained directly from the velocities generated during a molecular dynamics simulation, the model as we will illustrate, provides a direct route to the short-time dynamics of confined fluids. Unlike the VACF predicted from the real lobe of the INM DOS our model provides an improved prediction for the VACF particularly at short times, since it is accurate upto the fourth moment by construction. In addition a simple closed form expression for the VACF is obtained. We finally test the accuracy of the model by comparing the predicted relaxation times of the VACF, with those obtained from the INM theory and MD simulations.

II. THEORY

The normalized velocity autocorrelation function is defined as

$$\Psi(t) = \frac{\langle \mathbf{v}(0) \cdot \mathbf{v}(t) \rangle}{\langle |\mathbf{v}(0)|^2 \rangle}, \tag{1}$$

where $\langle |\mathbf{v}(0)|^2 \rangle = 3k_B T/m$ and k_B is the Boltzmann constant, T is the temperature, and m is the mass of the particle. The normalized VACF can be expressed as the even Fourier transform of the normalized DOS, $D(\omega)$ of the system,[25]

$$\Psi(t) = \int_0^\infty D(\omega) \cos(\omega t) d\omega. \tag{2}$$

In what follows, we give a brief introduction to INM analysis where the DOS is obtained within the harmonic approximation. Subsequently we derive an analytical expression for the VACF based on a γ distribution representation for the DOS. This expression for the VACF is obtained in terms of the parameters of the γ distribution. Next we propose a model for the VACF where we relate the parameters of the γ distribution to the second and fourth frequency moments of the DOS.

A. Instantaneous normal modes

As the details of the INM theory have been extensively discussed in the literature,[15,16,18] we briefly present the results relevant to our study. Consider a collection of N particles whose total potential energy is $\mathbf{U}(\mathbf{r}_1, \mathbf{r}_2, \ldots, \mathbf{r}_N)$ where $\mathbf{r}_i$ is the position of the ith particle. If $\mathbf{R}(t)$ represents the

collective positions of a given configuration at time t then the potential energy $\mathbf{U}$ expanded around a neighboring configuration $\mathbf{R}(t=0) \equiv \mathbf{R}_0$ is[17]

$$\mathbf{U}(\mathbf{R}) = \mathbf{U}(\mathbf{R}_0) + \mathbf{F}(\mathbf{R}_0) \cdot (\mathbf{R} - \mathbf{R}_0) + (1/2)(\mathbf{R} - \mathbf{R}_0)$$
$$\cdot \mathcal{H}(\mathbf{R}_0) \cdot (\mathbf{R} - \mathbf{R}_0), \tag{3}$$

where the components of the force vector $\mathbf{F}(\mathbf{R}_0)$ and Hessian matrix $\mathcal{H}(\mathbf{R}_0)$ are $f_i = -(\partial \mathbf{U}/\partial r_i)|_{\mathbf{R}_0}$ and $h_{i,j} = (\partial^2 \mathbf{U}/\partial r_i \partial r_j)|_{\mathbf{R}_0}$, $i, j = 1, \ldots, 3N$, respectively.

The eigenvalues ω_α^2 are obtained by diagonalizing the Hessian $\mathcal{H}$ for the system of particles at a particular configuration $\mathbf{R}_0$. Since the system is not in a global potential energy minimum, eigenvalues can be either positive or negative, giving rise to real and imaginary frequencies, ω_α. The INM density of states is the ensemble or time averaged distribution of frequencies obtained after averaging over many configurations $\mathbf{R}_0$ during a simulation. The normalized INM DOS is given by

$$D(\omega) = \left\langle \frac{1}{3N} \sum_{\alpha=1}^{3N} \delta[\omega - \omega_\alpha(\mathbf{R}_0)] \right\rangle_{\mathbf{R}_0}. \tag{4}$$

Since the harmonic approximation is applied to an instantaneous configuration of a liquid the INM DOS contains both real and imaginary frequencies, which are referred to as the stable and unstable modes of the system. Representing the imaginary frequencies as $i\omega$, Eq. (2) can be written as

$$\Psi(t) = \frac{\int [D_r(\omega)\cos(\omega t) + D_i(\omega)\cosh(\omega t)] d\omega}{\int D(\omega) d\omega}, \tag{5}$$

where $D_r(\omega)$ and $D_i(\omega)$ represent the contributions from the real and imaginary components of the INM DOS, respectively.

The presence of $\cosh(\omega t)$ in Eq. (5) leads to divergence of the VACF (Ref. 18) and hence should be considered only when one is interested in the time correlation function at very short times. On discarding the imaginary lobe of the INM DOS, the normalized VACF obtained from the real lobe is

$$\Psi_r(t) = \frac{\int_0^\infty D_r(\omega)\cos \omega t \, d\omega}{\int_0^\infty D_r(\omega) d\omega}. \tag{6}$$

B. VACF from γ distribution

In this work, we propose that the real lobe of the INM DOS can be represented by the normalized γ distribution,

$$G(\omega) = \frac{\alpha^m}{\Gamma(m)} \omega^{m-1} e^{-\alpha\omega} \quad \text{for } m > 1, \quad \alpha > 0, \tag{7}$$

where α and m are the two parameters of the model, which are related to the mean, m/α and variance, m/α^2 of the distribution, and $\Gamma(m)$ is the Gamma function. The choice of the γ distribution is motivated by the observation that the distribution captures the essential features that are typically present in distributions obtained from the INM DOS analysis. The real lobe of the INM DOS is zero at $\omega=0$. Further the distributions are antisymmetric about the peak frequency

with a long tail toward higher frequencies. Since the self-diffusivity is the zero frequency limit of the density of states $D(\omega)$, a model based on the γ distribution for the real lobe will predict a vanishing self-diffusion coefficient.

The expression for the normalized VACF of Eq. (6), on representing the real lobe of the INM DOS as a γ distribution given by Eq. (7), is

$$\Psi_r(t)=\frac{\alpha^m}{\Gamma(m)}\,\mathrm{Re}\left[\int_0^\infty \omega^{m-1}e^{-\omega(\alpha+it)}d\omega\right]. \qquad (8)$$

The integral which appears in Eq. (8) can be evaluated analytically[26] resulting in the following closed form expression for the VACF:

$$\Psi_r(t)=\left[1+\left(\frac{t}{\alpha}\right)^2\right]^{-m/2}\cos\left[m\arctan\left(\frac{t}{\alpha}\right)\right]. \qquad (9)$$

We note that the form for $\Psi_r(t)$ is an even function of time, satisfying the time reversal property of the VACF. The property that the VACF is an even function of time is a consequence of the definition [Eq. (2)] being a cosine transform and is independent of the choice of $G(\omega)$. As a consequence all odd moments of the VACF vanish at the origin.

Before concluding this section we note that an analytical expression can be obtained for the contribution to the VACF from the imaginary lobe of the INM DOS if $D_i(\omega)$ is represented by a γ distribution. The expression for the VACF from the imaginary lobe is

$$\Psi_i(t)=\frac{\int_0^\infty D_i(\omega)\cosh\omega t\,d\omega}{\int_0^\infty D_i(\omega)d\omega}. \qquad (10)$$

Utilizing the relations from Eq. (7), it can be shown that

$$\Psi_i(t)=\frac{\alpha^m}{2\Gamma(m)}\int_0^\infty \omega^{m-1}e^{-\alpha\omega}(e^{\omega t}+e^{-\omega t})d\omega$$

$$=\frac{1}{2\left[1+\dfrac{t}{\alpha}\right]^m}+\frac{1}{2\left[1-\dfrac{t}{\alpha}\right]^m}\quad\text{for } t<\alpha. \qquad (11)$$

For $t\geq\alpha$ the integral diverges and cannot be evaluated analytically. Evaluating the moments from Eq. (11), we observe that the odd moments vanish, consistent with the fact that VACF is an even function of time.

C. Proposed model for VACF

Although our results will later indicate that γ distribution provides an accurate representation of the real lobe INM DOS, the utility of such a description depends on developing a model to predict the parameters α and m which appear in the expression for VACF developed above [Eq. (9)]. It is known that the VACF obtained from the INM DOS is accurate upto the fourth moment only when both lobes of the INM DOS are used.[18] However, the resulting VACF is divergent. In order to avoid the divergence in the VACF it is customary to evaluate the VACF from the INM DOS corresponding to the real lobe alone.[18] Although the resulting VACF computed in this manner is well behaved, neglecting the contributions from the imaginary lobe results in moments

that are larger than the actual moments of the system. Hence VACFs predicted from the real lobe of the INM DOS generally tend to relax faster than the actual VACF. In this section we seek to develop a model that is both well behaved at long times and by construction is accurate upto the fourth moment of the DOS. The starting point for such a development is based on short-time expansions of the time correlation function. Noting that the VACF is an even function of time, the Taylors series expansion around $t=0$ is

$$\Psi(t)=1-\frac{t^2}{2!}\,\omega_v^2+\frac{t^4}{4!}\,\omega_v^4-\cdots, \qquad (12)$$

where

$$\omega_v^{2n}=(-1)^n\left(\frac{d^{2n}\Psi(t)}{dt^{2n}}\right)_{t=0},\qquad n=1,2,\dots. \qquad (13)$$

Using a series expansion for $\cos\omega t$, Eq. (2) for the VACF can be expressed as

$$\Psi(t)=1-\frac{t^2}{2!}\frac{\int D(\omega)\omega^2 d\omega}{\int D(\omega)d\omega}+\frac{t^4}{4!}\frac{\int D(\omega)\omega^4 d\omega}{\int D(\omega)d\omega}-\cdots. \qquad (14)$$

Comparing Eq. (14) with Eq. (12) the expression for the even moments of the VACF in terms of the DOS are

$$\omega_v^{2n}=\frac{\int D(\omega)\omega^{2n}d\omega}{\int D(\omega)d\omega},\qquad n=1,2,\dots. \qquad (15)$$

The frequency moments take a central place in theories concerned with the dynamics of the liquid state. They can be obtained directly from the pair correlation function in the case of a bulk fluid or more generally from particle velocities generated during a MD simulation by using Eq. (13). The corresponding expressions for the frequency moments ω_v^2 and ω_v^4 in terms of the particle velocities are given later in the text. Equation (15) which relates the moments to the DOS is of little utility unless an expression of the DOS is known. Since the VACF is the function that one seeks to obtain, the DOS is generally an unknown quantity. In this paper we model the DOS of the system [Eq. (2)] by a γ distribution which results in Eq. (9) for the VACF. With the requirement that the VACF is accurate upto the fourth moment, relationships between the parameters of the γ distribution and the frequency moments are obtained. The expression for the nth order moment of the γ distribution,

$$\omega_v^n=\int_0^\infty \frac{\alpha^m}{\Gamma(m)}\,\omega^{m-1+n}e^{-\alpha\omega}d\omega$$

$$=\frac{\Pi_{k=0}^{n-1}(m+k)}{\alpha^n},\qquad n=1,2,\dots, \qquad (16)$$

where we have used the recurrence relation, $\Gamma(m+n)=(m+n-1)\Gamma(m+n-1)$. Since only the even moments [Eq. (15)] are required while developing short-time expansions for the VACF, the second and fourth moment of the VACF, from Eq. (16) are

$$\omega_v^2 = \frac{m(m+1)}{\alpha^2}, \tag{17}$$

and

$$\omega_v^4 = \frac{m(m+1)(m+2)(m+3)}{\alpha^4}. \tag{18}$$

Casting Eqs. (17) and (18) as a quadratic for m, the corresponding roots will be of different signs if $[\omega_v^4 - (\omega_v^2)^2] > 0$. This condition is satisfied for all the state points we have studied. The expression for the *positive* value of m in terms of ω_v^2 and ω_v^4 and the positive value of α corresponding to this value of m are, respectively,

$$m = \frac{[5(\omega_v^2)^2 - \omega_v^4] + \sqrt{[\omega_v^4 - 5(\omega_v^2)^2]^2 + 24(\omega_v^2)^2[\omega_v^4 - (\omega_v^2)^2]}}{2[\omega_v^4 - (\omega_v^2)^2]} \tag{19}$$

and

$$\alpha = \frac{\sqrt{4\omega_v^2[(\omega_v^2)^2 + \omega_v^4] + 2\omega_v^2\sqrt{[\omega_v^4 - 5(\omega_v^2)^2]^2 + 24(\omega_v^2)^2[\omega_v^4 - (\omega_v^2)^2]}}}{[\omega_v^4 - (\omega_v^2)^2]}. \tag{20}$$

Equations (19) and (20) provide the necessary relations that relate the parameters of the distribution to the frequency moments. The proposed model for the VACF is similar in spirit to the development of other models for the time correlation function which require the frequency moments as their primary input.[25] These theories are either based on proposing a form for the VACF or if a memory function approach is used one proposes a form for the memory kernel.[14,27] The fundamental difference in the model presented here is the proposition of a suitable form for the DOS itself. By construction the VACF is accurate upto the fourth moment and is nondivergent. This is an improvement over VACF predictions based only on the real lobe of the INM DOS.

D. Relaxation time

Since the INM analysis is in reality a theory developed for short times, a comparison of the relaxation time of the VACFs is expected to provide a quantitative measure of the ability of the theory to capture the short-time dynamics of system. In addition the relaxation time is sometimes used as a parameter while developing models for the VACF.[25] A convenient definition of τ, the relaxation time, is[28,29]

$$\tau = 2\int_0^\infty [\Psi_r(t)]^2 dt. \tag{21}$$

Substituting the form of VACF [Eq. (9)] into Eq. (21) we obtain an analytical expression for the relaxation time in terms of the parameters of the model.

$$\tau_M = \frac{\sqrt{\pi}}{2}\alpha\frac{\Gamma\left(m - \frac{1}{2}\right)}{\Gamma m}. \tag{22}$$

III. SIMULATION DETAILS

Figure 1(a) illustrates a structured pore of width H where the pore wall consists of discrete particles, and Fig. 1(b) illustrates a smooth walled pore where the interaction of the

wall with the fluid molecules is only in the z direction. Both pores are infinite in the x-y plane, but finite in the z direction. For a confined fluid, the total potential energy $U = U_{ff} + U_{fw}$, where U_{ff} is the total fluid-fluid interaction energy and U_{fw} is the total fluid-wall interaction. For a system with N fluid particles with pairwise additive potentials,

$$U_{ff} = \sum_{i=1}^{N-1}\sum_{j>i} u(r_{ij}). \tag{23}$$

The fluid-fluid interactions are assumed to be Lennard-Jones (LJ) 12-6 potential,

$$u(r_{ij}) = 4\epsilon_{ff}\left[\left(\frac{\sigma_{ff}}{r_{ij}}\right)^{12} - \left(\frac{\sigma_{ff}}{r_{ij}}\right)^6\right], \tag{24}$$

where ϵ_{ff} and σ_{ff} are the LJ potential parameters. For the structured pore, fluid-wall interactions are modeled using the
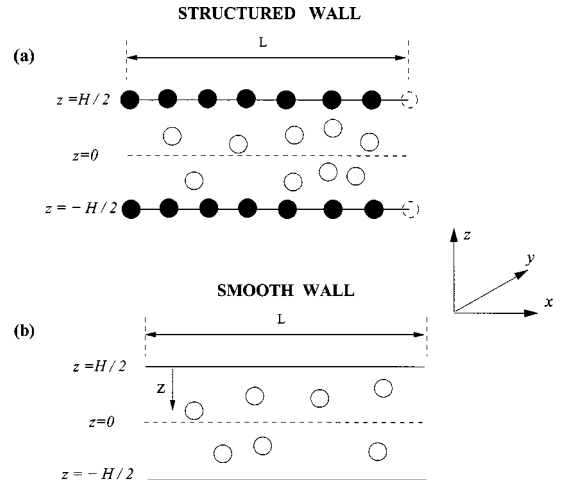

FIG. 1. Schematic of (a) structured and (b) smooth slit pore indicating the pore width H and periodic box length L. Periodic boundary conditions are applied in the x and y directions.

Quantity	Reduced unit
Potential energy	$u^* = u/\epsilon_{ff}$
Slit width	$H^* = H/\sigma_{ff}$
Box length	$L^* = L/\sigma_{ff}$
Time	$t^* = t\sqrt{\epsilon_{ff}/m\sigma_{ff}^2}$
Temperature	$T^* = kT/\epsilon_{ff}$
Density	$\rho^* = \rho\sigma_{ff}^3$
Velocity	$v^* = v\sqrt{m/\epsilon_{ff}}$
Force	$F^* = F\sigma_{ff}/\epsilon_{ff}$
Frequency	$\omega^* = \omega\sqrt{m\sigma_{ff}^2/\epsilon_{ff}}$

12-6 LJ potential with the potential parameters ϵ_{fw} and σ_{fw}. The total fluid-wall potential for the structured pore consisting of N_w wall particles is

$$U_{fw} = \sum_{i=1}^{N}\sum_{j=1}^{N_w} u(r_{ij}). \qquad (25)$$

Each wall consisted of 200 particles arranged in a fcc lattice. This corresponds to a pore of periodic box length $L^* = 14.14$. For the smooth pore, fluid-wall interactions were modeled using a 10-4 potential,[14] where the interaction is only a function of the normal distance of the fluid particle from the wall.

The fluid-fluid and fluid-wall LJ interaction parameters used in this study correspond to those of argon ($\sigma_{ff} = \sigma_{fw} = 3.405$ Å and $\epsilon_{ff}/k_B = \epsilon_{fw}/k_B = 120$ K). All results are reported in reduced units as shown in Table I. Simulations were conducted in the NVE ensemble for 100 000 time steps, with 50 000 equilibration steps. For each step, $\Delta t^* = 0.004 \approx 0.008$ ps. Four hundred configurations spaced equally by 125 time steps were used to calculate the INM DOS. VACFs were computed from particles velocities output at every time step and time origins were shifted every ten steps.[28,30] Simulations were carried out for slit widths which can accommodate two, three, and four layers inside the pore. The details of the simulation for both the structured and smooth pores are given in Table II. In Table II, $\rho^* = \langle N \rangle / V^*$ where the dimensionless pore volume V^* is computed using the pore width as illustrated in Fig. 1.

A. Expression for Hessian

For a system of N particles in a structured pore, the Hessian $\mathcal{H}$ is a $3N \times 3N$ matrix from which the instantaneous

ρ^*	H^*	L^*	N
	Structured pore		
0.5	2.75	14.14	274
0.6	4.00	14.14	479
0.68	4.40	14.14	598
	Smooth pore		
0.54	2.75	14.14	296
0.6	4.00	14.14	479

normal modes are obtained. An element of the Hessian matrix $\mathcal{H}$, for interaction between two particles i and j, such that $i \neq j$, is[31]

$$h_{3(i-1)+\alpha, 3(j-1)+\beta} = -\frac{\delta_{\alpha\beta}}{r_{ij}}\frac{du(r_{ij})}{dr_{ij}}$$
$$- \frac{(r_{i\alpha}-r_{j\alpha})(r_{i\beta}-r_{j\beta})}{r_{ij}}$$
$$\times \frac{d}{dr_{ij}}\left(\frac{1}{r_{ij}}\frac{du(r_{ij})}{dr_{ij}}\right). \qquad (26)$$

In the above expression, $i, j = 1,...,N$ and $\alpha, \beta = 1, 2, 3$ which correspond to the three Cartesian coordinates, $r_{i\alpha} = x_i$, y_i, or z_i, and $u(r_{ij})$ is the interatomic potential between particles i and j separated by a distance r_{ij}. Between two distinct components of the same particle ($i = j$) the elements which form a diagonal block of 3×3 elements in $\mathcal{H}$ are

$$h_{3(i-1)+\alpha, 3(i-1)+\beta} = -\sum_{i\neq j} h_{3(i-1)+\alpha, 3(j-1)+\beta}$$
$$- \sum_{w=1}^{N_w} \partial_\alpha\partial_\beta u(r_{iw}), \qquad (27)$$

where ∂_α represents the partial derivative with respect to α.

At any instantaneous configuration generated during the MD simulation, the eigenvalues of $\mathcal{H}$ are obtained. The square roots of the eigenvalues give the characteristic frequencies of the system. The normalized INM DOS, $D(\omega)$ is the distribution obtained by binning these frequencies and taking an average over a number of different configurations.

B. Moments of the VACF

From Eq. (13), the moments can be directly obtained from the particle velocities[25] generated during the MD simulation. The second moment is computed using

$$\omega_v^2 = \frac{\langle \dot{v}_x(0)^2 + \dot{v}_y(0)^2 + \dot{v}_z(0)^2 \rangle_{t,N}}{\langle v_x(0)^2 + v_y(0)^2 + v_z(0)^2 \rangle_{t,N}}, \qquad (28)$$

where v_x, v_y, and v_z are the single particle velocities in Cartesian coordinates, and $\langle \cdots \rangle_{t,N}$ denotes time origins and particle averaging. The fourth moment is

$$\omega_v^4 = \frac{\langle \ddot{v}_x(0)^2 + \ddot{v}_y(0)^2 + \ddot{v}_z(0)^2 \rangle_{t,N}}{\langle v_x(0)^2 + v_y(0)^2 + v_z(0)^2 \rangle_{t,N}}. \qquad (29)$$

Derivatives of the velocities were computed numerically at every time step using a first-order finite difference scheme.

IV. RESULTS AND DISCUSSION

A. Velocity autocorrelation function

We compare the VACFs from MD simulations (VACF_{MD}) with VACFs obtained from the real lobe of INM DOS (VACF_{INM}) and from the proposed model (VACF_{M}). The parameters m and α [Eqs. (19) and (20)] of the model used in the expression for the VACF_{M} [Eq. (9)] are given in Table III. For purposes of discussion we will refer to the portion of the VACF from zero time till the zero crossing as "short times" and for subsequent portions upto $t \approx 1$ ps as

TABLE III. Parameters of the proposed model for a structured pore obtained from Eqs. (19) and (20) for different temperatures. α is reported in units of reduced time.

H^*	T^*	ρ^*	m	α
2.75	0.9	0.5	2.358	0.1678
2.75	1.2	0.5	2.163	0.1459
2.75	1.5	0.5	2.030	0.1315
4.00	0.9	0.6	2.037	0.1545
4.00	1.2	0.6	1.976	0.1356
4.00	1.5	0.6	1.751	0.1191
4.40	0.9	0.68	2.517	0.1607
4.40	1.2	0.68	2.273	0.1371
4.40	1.5	0.68	2.104	0.1215

FIG. 3. Comparison of proposed model VACF_M [Eq. (9) with parameters obtained from frequency moments using Eqs. (19) and (20)] and VACF_G [Eq. (9) with fitted parameters from INM DOS] and VACF_{INM} [Eq. (6)] with VACF_{MD} for a two layer structured pore ($H^*=2.75$ and $\rho^*=0.5$). Divergent VACF from both lobes of INM ($\cdots$) and the corresponding γ distribution model ($\bigcirc$) are also shown.

"intermediate times." Unless otherwise stated, all results will correspond to the structured pore. Results are reported for structured pores for pore widths that can accommodate two, three, and four fluid layers. The corresponding density distributions for these systems for a fixed pore density as a function of temperature are shown in Fig. 2. For the temperature ranges investigated in this study, an increase in temperature only marginally increases the spread in the density distribution.

Comparison of the predicted VACFs with MD results for a two layer system are shown in Fig. 3. We first focus on the predictions of the VACFs obtained from the INM DOS analysis and illustrate that the INM DOS can be suitably modeled by γ distributions. In Fig. 3 the VACFs computed from the γ distribution representation for the INM DOS, where the parameters are obtained as best fits to the INM DOS (VACF_G) data, are compared with the VACF_{INM}. The divergent VACF obtained from both lobes of the INM DOS are shown as well. The VACF predictions illustrate that the γ distribution is able to provide an accurate representation of the INM DOS. The INM DOS for both real and imaginary lobes are shown in Fig. 4 where in all the pores which considered the γ distributions are seen to provide an excellent fit
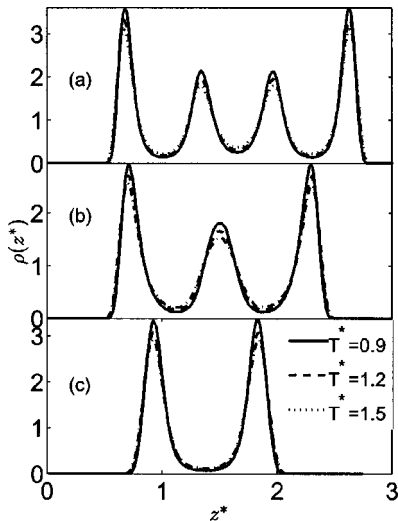
to the INM DOS data. The accuracy of these representations is reflected in the close similarities in the predicted VACFs shown for the two layered situation in Fig. 3. We point out that VACF_{INM} is seen to underpredict the magnitude of the VACF at short times prior to the negative regions in the VACF. However, the predictions are in extremely good agreement at intermediate times, capturing the broad negative regions typically observed in VACFs of confined fluids. The loss of information at short times results from neglecting imaginary lobes of the INM DOS and has been observed in other INM DOS investigations for bulk fluids[32] and rare gases in zeolites.[23] We next compare the VACF predicted from the proposed model (VACF_M) with VACF_{INM} and

FIG. 2. Density distributions for a fluid inside a structured pore at slit widths of (a) $H^*=4.40$, (b) $H^*=4.0$, (c) $H^*=2.75$ at temperatures of $T^*=0.9$, 1.2, 1.5, respectively.

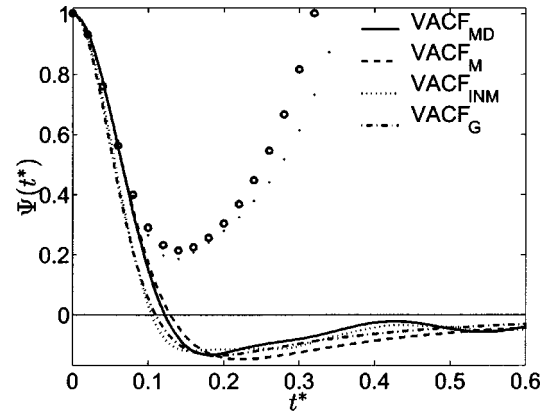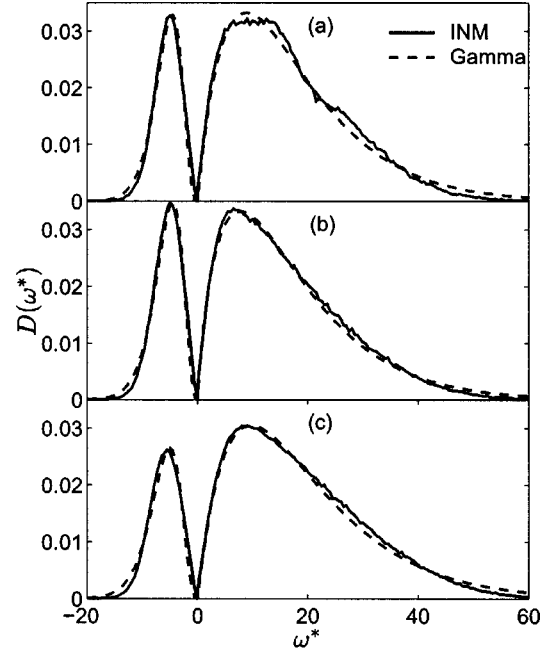FIG. 4. INM DOS (solid lines) for structured pores at slit widths (a) $H^*=2.75$ (two layer system), (b) $H^*=4.00$ (three layer system), and (c) $H^*=4.40$ (four layer system). Best fit γ representations (dashed lines) for real and imaginary lobes are also shown.
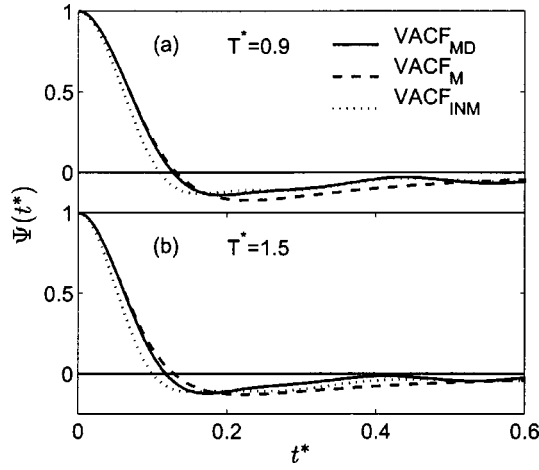
FIG. 5. Comparison of VACF$_M$ with VACF$_{INM}$ and VACF$_{MD}$ two layered system ($H^* = 2.75$) at (a) $T^* = 0.9$ and (b) $T^* = 1.5$.

VACF$_{MD}$. The accuracy of VACF$_M$ upto the fourth moment is reflected in the excellent agreement with VACF$_{MD}$ at short times. However, at intermediate times VACF$_M$ results in a larger negative region in the VACF when compared with both VACF$_{MD}$ and VACF$_{INM}$. The larger negative regions at intermediate times are a consequence of the zero diffusivity character of the model.

As the comparisons between the predictions of the VACF$_{INM}$ and VACFs from the fitted γ distributions are quantitatively similar to those illustrated in Fig. 3 we do not illustrate the latter VACFs for the other pore conditions investigated. In order to study the effect of temperature, VACFs in the two layered regime at $T^* = 0.9$ and $T^* = 1.5$ are illustrated in Figs. 5(a) and 5(b), respectively. The pore density is similar to that used in Fig. 3. There is an excellent
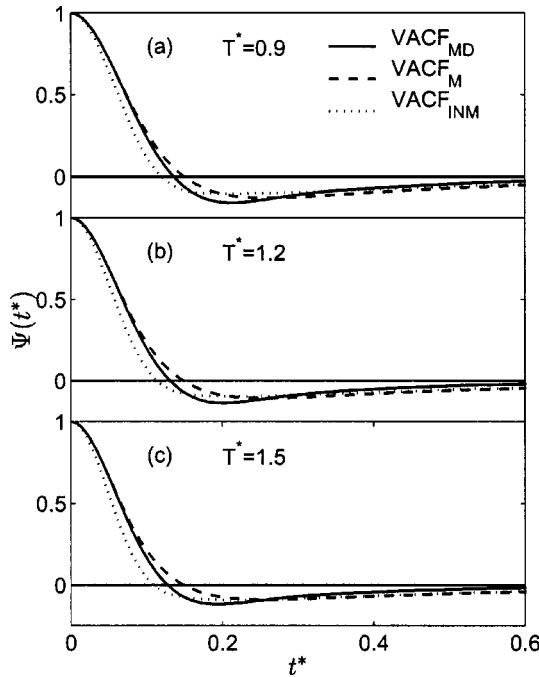

FIG. 6. Comparison of VACF$_M$ and VACF$_{INM}$ with VACF$_{MD}$ for a three layer system ($H^* = 4.00$) at (a) $T^* = 0.9$, (b) $T^* = 1.2$, and (c) $T^* = 1.5$.
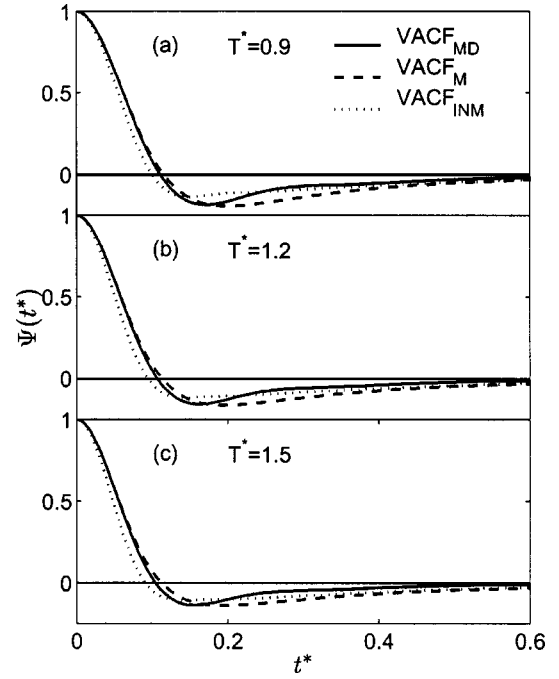

FIG. 7. Comparison of VACF$_M$ and VACF$_{INM}$ with VACF$_{MD}$ for a four layer system ($H^* = 4.40$) at (a) $T^* = 0.9$, (b) $T^* = 1.2$, and (c) $T^* = 1.5$.

match between VACF$_{MD}$ and VACF$_M$ and for short times both the VACFs are indistinguishable. At intermediate times VACF$_M$ slightly underpredicts VACF$_{MD}$. The agreement of both VACF$_M$ and VACF$_{INM}$ is seen to improve as the temperature is lowered. The trends observed in VACF$_{INM}$ are similar to those observed earlier (Fig. 3) where the mismatch occurs at short times and improved performance is observed at intermediate times. The results for pore widths which accommodate three and four fluid layers are shown in Figs. 6 and 7, respectively. In each case we have studied the performance of the models for three different temperatures. The qualitative features of the comparison are similar to that observed for the two layer system.
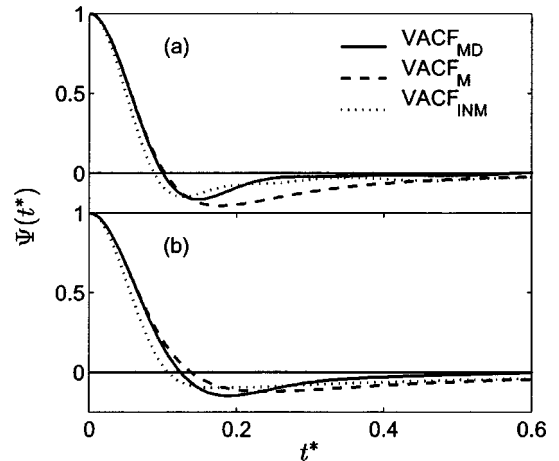

FIG. 8. (a) Comparison of VACF$_M$ and VACF$_{INM}$ with VACF$_{MD}$ for a *smooth pore* (a) two ($H^* = 2.75$) and (b) three ($H^* = 4.00$) layered system at $T^* = 1.2$.
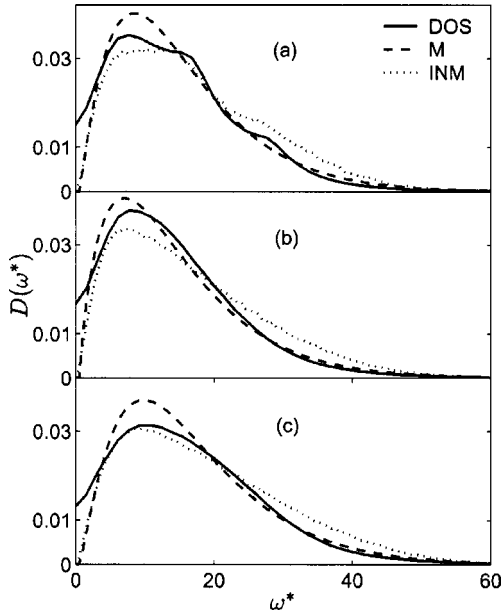
FIG. 9. DOS for a confined fluid in a structured pore at slit widths corresponding to (a) two layer ($H^* = 2.75$), (b) three layer ($H^* = 4.00$), and (c) four layer ($H^* = 4.40$). Comparison against the proposed model (M) and real lobe of INM DOS are also shown.

The results for a two layer system in a smooth pore are shown in Fig. 8(a). Although the best agreement with MD results till the minima is seen by VACF_M the range of negative correlations are overpredicted by the model. The results for a three layer system of the smooth pore are shown in Fig. 8(b). The VACF_M matching with MD results till the minima with a slight overprediction of the minima, and VACF_{INM} exhibiting a mismatch for the short times and underpredicting the minima.

B. Density of states

As the proposed model is based on a γ distribution for the DOS it is instructive to compare it with the DOS obtained from VACF_{MD} [Eq. (2)] and the real lobe of INM DOS. The DOS is obtained by a Fourier transform of VACF_{MD} whose zero frequency limit is the self-diffusivity of the system. The DOS for two-, three-, and four-layered systems are compared in Fig. 9. The accuracy of the proposed γ

model upto the fourth moment is reflected in the excellent match between the DOS of the proposed model and the actual DOS at higher frequencies. INM DOS, on the other hand, tends to overpredict the actual DOS values at higher frequencies. These trends observed in the DOS are consistent with the predicted behavior in the corresponding VACFs at short times. It is interesting to note that both the DOS from the model and the INM DOS are able to capture the peak frequency in the DOS rather accurately. We note that the peak frequency can be expressed in terms of the model parameters as $(m-1)/\alpha$.

C. Relaxation time

In Table IV relaxation times are reported for the various pores investigated in this study. τ^*_{MD} and τ^*_{INM} are obtained by numerically integrating Eq. (21) with VACF_{MD} and VACF_{INM}, respectively, and τ^*_M is obtained from the analytical expression given in Eq. (22).

In all cases the relaxation times predicted from the proposed model are in better agreement with MD results. However, the model tends to overestimate the relaxation time while the INM DOS underestimates the relaxation time. These trends in the relaxation times are reflected in the corresponding VACFs discussed earlier, see, for example, Fig. 6. The inaccuracy of the VACF_{INM} at short times is due to the quicker decay in the VACF when compared with the VACF_{MD}. The faster decay is reflected in the smaller relaxation times in τ^*_{INM}. This is a consequence of neglecting the imaginary lobe while computing the VACFs. Since VACF_M is constructed such that it is exact upto the fourth moment, there is an improved agreement between τ^*_M and τ^*_{MD}. Note that although VACF_M underpredicts the actual VACF at intermediate times, the improved performance over VACF_{INM} at short times improves the predicted relaxation time. The results for the percentage deviations for relaxation time corresponding to the numerical values shown in Table IV are plotted in Fig. 10 for all the state points studied. In the figure x-axis values of n correspond to the value of n given in Table IV. For all the state points, the maximum deviation in case of the model prediction is less than 7%, whereas the INM DOS are in error by as much as 14%. It can be also observed that

TABLE IV. Comparison of relaxation times τ^* for structured pore at different temperatures. τ^*_{MD} and τ^*_{INM} are obtained integrating VACF_{MD} and VACF_{INM} [Eq. (21)] and τ^*_M from Eq. (22). The values shown in brackets for selected state points are the results from best fit γ distributions to the INM DOS. The percent differences between τ^*_M and τ^*_{INM} with τ^*_{MD} results are shown as $\% \Delta \tau_{\text{MD},M}$ and $\% \Delta \tau_{\text{MD,INM}}$, respectively. n indexes all the state points studied (Fig. 10).

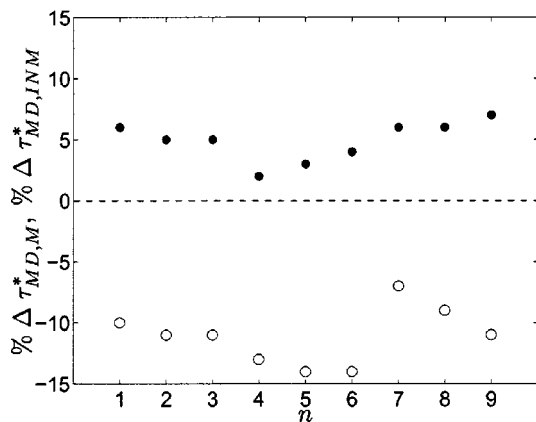| n	H^*	T^*	ρ^*	τ^*_M	τ^*_{INM}	τ^*_{MD}	$\% \Delta \tau^*_{\text{MD},M}$	$\% \Delta \tau^*_{\text{MD,INM}}$
1	2.75	0.9	0.5	0.116	0.098	0.109	6	10
2	2.75	1.2	0.5	0.108	0.092(0.088)	0.103	5	11
3	2.75	1.5	0.5	0.102	0.086	0.097	5	11
4	4.00	0.9	0.6	0.119	0.101	0.116	2	13
5	4.00	1.2	0.6	0.110	0.093(0.091)	0.107	3	14
6	4.00	1.5	0.6	0.104	0.086	0.100	4	14
7	4.40	0.9	0.68	0.106	0.090	0.100	6	7
8	4.40	1.2	0.68	0.097	0.083(0.079)	0.091	6	9
9	4.40	1.5	0.68	0.092	0.076	0.086	7	11

FIG. 10. Percent differences between τ_M^* and τ_{MD}^* (●) and τ_{INM}^* and τ_{MD}^* (○) for structured pores. The x axis represents different state points studied with values of n corresponding to the data shown in Table IV.

the model overpredicts the MD results, whereas the INM DOS results underpredict the same.

V. SUMMARY AND CONCLUSIONS

In this paper INM theory has been used to model the short-time dynamics of fluids confined in slit-shaped pores and a model for the VACF, based on a γ representation for the DOS, has been proposed and evaluated. The two parameters of the γ distribution are related to the second and fourth moment of the actual DOS of the system. Hence the model is accurate upto the fourth moment by construction and in this aspect presents an improvement over the time correlation predictions from the real lobe of the INM DOS. The performance of the model is evaluated by comparing the predicted VACF with those obtained from molecular dynamics simulations and from INM analysis. Comparisons have been carried out for fluids confined in structured pores over a wide range of confinement and temperatures. The model is seen to capture the short-time behavior of the VACF extremely accurately and in this region is superior to the predictions of the VACF obtained from the real lobe of the INM DOS. As a result the predicted relaxation times of the model are in closer agreement with the molecular dynamics results. More significantly the model results in closed form expressions for the VACF and relaxation times.

The model development proposed here is similar in spirit to other models for the liquid state which attempt to model the VACF with frequency moments as the primary input. However, unlike other models where one either proposes a form for the memory kernel or the VACF, we propose a form for the density of states. The model is built on the observation that the γ distribution captures the essential features of the real lobe of the INM DOS over a wide range of pore fluid conditions. Although we do not have an independent theory to justify the γ distribution, our results indicate that the γ distribution results in VACFs which are extremely accurate at short times. The utility of the model is further enhanced by the reliable prediction of relaxation times, which can in turn be used as inputs into models aimed at obtaining long-time

diffusive behavior. These models are based on proposing a suitable form for the VACF or can be developed from kinetic theory.[33,34] We are currently exploring these approaches for bulk and confined fluids.

In conclusion our study suggests that the INM analysis is appropriate for studying short-time dynamics of strongly inhomogeneous systems that arise when fluids are confined in slit-shaped pores. We point out that the frequency moments used as inputs into the proposed model can also be obtained from an INM analysis. Hence the proposed model can be used in conjunction with the INM theory which requires as input only particle configurations from a system that is in equilibrium. However, unlike the INM theory which is better suited for dense and supercooled systems our model is expected to be applicable over a wider range of fluid conditions.

[1] J. N. Israelachvili, *Intermolecular and Surface Forces: With Applications to Colloidal and Bioligical Systems* (Academic, London, 1985).
[2] C. Ghatak and K. G. Ayappa, Phys. Rev. E **64**, 051507 (2001).
[3] J. Klein and E. Kumacheva, J. Chem. Phys. **108**, 6996 (1998).
[4] L. A. Demirel and S. Granick, Phys. Rev. Lett. **77**, 2261 (1996).
[5] A. Mukhopadhyay, J. Zhao, S. C. Bae, and S. Granick, Phys. Rev. Lett. **89**, 136103 (2002).
[6] J. J. Magda, M. Tirrell, and H. T. Davis, J. Chem. Phys. **83**, 1888 (1985).
[7] M. Schoen, J. H. Cushman, D. J. Diestler, and C. L. Rhykerd, J. Chem. Phys. **88**, 1394 (1988).
[8] S. A. Somers and H. T. Davis, J. Chem. Phys. **96**, 5389 (1992).
[9] P. Bordarier, B. Rousseau, and A. H. Fuchs, Mol. Simul. **17**, 199 (1996).
[10] M. Schoen, *Computer Simulation of Condensed Phases in Complex Geometries* (Springer, Berlin, 1993).
[11] H. T. Davis, J. Chem. Phys. **86**, 1474 (1987).
[12] T. K. Vanderlick and H. T. Davis, J. Chem. Phys. **87**, 1791 (1987).
[13] J. M. D. Macelroy and S. H. Suh, Mol. Simul. **2**, 313 (1989).
[14] S. H. Krishnan and K. G. Ayappa, J. Chem. Phys. **118**, 690 (2003).
[15] R. M. Stratt, Acc. Chem. Res. **28**, 201 (1995).
[16] T. Keyes, J. Phys. Chem. A **101**, 2921 (1997).
[17] G. Seeley and T. Keyes, J. Chem. Phys. **91**, 5581 (1989).
[18] M. Buchner, B. M. Ladanyi, and R. M. Stratt, J. Chem. Phys. **97**, 8522 (1992).
[19] J. D. Gezelter, E. Rabani, and B. J. Berne, J. Chem. Phys. **107**, 4618 (1997).
[20] T. Keyes, W. X. Lee, and U. Zurcher, J. Chem. Phys. **109**, 4693 (1998).
[21] J. D. Gezelter, E. Rabani, and B. J. Berne, J. Chem. Phys. **109**, 4695 (1998).
[22] J. Chowdhary and T. Keyes, Phys. Rev. E **65**, 026125 (2002).
[23] S. Kar and C. Chakravarty, J. Phys. Chem. B **104**, 709 (2000).
[24] C. Rajappa, S. Bandyopadhyay, and S. Yashonath, Bull. Mater. Sci. **20**, 845 (1997).
[25] J. Boon and S. Yip, *Molecular Hydrodynamics* (Dover, New York, 1991).
[26] I. S. Gradshteyn and I. M. Ryzhik, *Table of Integrals, Series and Products* (Academic, London, 1994).
[27] D. M. Heyes and J. G. Powles, Mol. Phys. **71**, 781 (1990).
[28] J. M. Haile, *Molecular Dynamics Simulation* (Wiley, New York, 1992).
[29] R. Zwanzig and N. K. Ailwadi, Phys. Rev. **182**, 280 (1969).
[30] J. W. Allen and D. J. Diestler, J. Chem. Phys. **73**, 4597 (1980).
[31] R. A. LaViolette and F. H. Stillinger, J. Chem. Phys. **83**, 4079 (1985).
[32] G. Seeley, T. Keyes, and B. Madan, J. Phys. Chem. **96**, 4074 (1992).
[33] D. M. Heyes, J. G. Powles, and G. Rickayzen, Mol. Phys. **100**, 595 (2002).
[34] H. T. Davis, in *Fundamentals of Inhomogeneous Fluids*, edited by D. Henderson (Dekker, New York, 1992).